FOUNDATIONS OF BURKINA FASO'S GREAT GREEN WALL: VEGETATION GROWTH IN THE SAHEL SINCE 1990

by

Nicolas Karwowski

A Major Research Paper

presented to Ryerson University

in partial fulfilment of the requirements for the degree of

Master of Spatial Analysis

in the Program of Spatial Analysis

Toronto, Ontario, Canada

© Nicolas Karwowski 2021

Author's Declaration

I hereby declare that I am the sole author of this research paper.

I authorize Ryerson University to lend this research paper to other institutions or individuals for the purpose of scholarly research.

_____

I further authorize Ryerson University to reproduce this research by photocopying or by other means, in total or in part, at the request of other institutions or individuals for the purpose of scholarly study.

_____

Abstract

The importance of the Sahel region as a barrier between the lush lands of sub-Saharan Africa and the unforgiving Sahara Desert has been known for decades. However, this region has not remained impervious to desertification, a process in which vegetation ceases to grow due to changing climate and poor agriculture practices, amongst other factors. In 2006, the African Union conceived a plan to halt the advancing desert, a wall of greenery stretching from coast to coast dubbed the Great Green Wall. Since its inception, the ambitious project has been widely criticized for its slow progression, and its utility has been questioned. This study is seeking to quantify vegetation growth before the Great Green Wall's launch and after it to evaluate the importance of the project. With the Landsat satellites imaging the Earth since 1972, a large archive of imagery is available for examination. By conducting a change detection analysis on images acquired between 1990 and 2020, vegetation growth can be measured through the project's duration as well as prior to it. Image differencing was used to detect vegetation loss and growth in four time intervals since 1990. These results were then coupled with unsupervised classifications that identified land uses. Between 1990 and 2002, a period preceding the Great Green Wall, massive vegetation loss was observed. The following period, between 2002 and 2007, saw massive growth, undoing much of previous time interval's loss. While growth was again slightly outpaced by loss between 2007 and 2014, 2014 to 2020 saw vegetation growth soaring again. While the study's methods allowed for the quantification of vegetation change between 1990 and 2020, a correlation between the Great Green Wall and these findings cannot be established without additional data such as precipitation records or local observations.

Acknowledgements

I would like to issue a special thanks to Professor K. Wayne Forsythe for his support through the research process as well as through countless remote sensing classes in both the Geographic Analysis undergraduate program and the Masters of Spatial Analysis. Thank you to Laura, my friends and family, for their constant encouragement and belief in me through this complicated year. I would like to thank the rest of the Ryerson University Geography and Environmental Studies Department faculty and the Geospatial Map and Data Centre for their unending devotion to guide and mentor students despite the immense challenges faced through 2020 – 2021.

Table of Contents

Author's Declaration ii

Abstract iii

Acknowledgements iv

Table of Contents v

List of Figures vii

List of Tables viii

List of Acronyms ix

CHAPTER 1: Introduction 1

1.1 The Sahel 1

1.2 The Great Green Wall 4

1.3 Research Objectives 8

1.4 Study Area 9

CHAPTER 2: Data 12

2.1 The Landsat program 12

2.2 Preprocessing 17

CHAPTER 3: Methods 19

3.1 Image Differencing 19

CHAPTER 4: Results & Discussion 32

4.1 1990 to 2002 32

4.2 2002 to 2007 34

4.3 2007 to 2014 356

4.4 2014 to 2020 376

4.5 Implications and Discussion 378

Chapter 5: Conclusion 412

5.1 Limitations 42

References 44

List of Figures

Figure 1: The Sahel 2

Figure 2: Study Area in True Colour 11

Figure 3: NDVI 2020 20

Figure 4: NDVI Change 2014 - 2020 22

Figure 5: First Classfication Results 25

Figure 6: Second Classfication Results 26

Figure 7: NDWI 2020 28

Figure 8: Third Classification Results 30

Figure 9: Vegetation Change 1990 to 2002 33

Figure 10: Vegetation Change 2002 to 2007 35

Figure 11: Vegetation Change 2007 to 2014 37

Figure 12: Vegetation Change 2020 to 2020 39

Figure 13: Vegetation Change Chart 1990 to 2020 41

List of Tables

Table 1: Source Images & Omitted Images 16

Table 2: Accuracy Assessment for the First Classification 24

Table 3: Accuracy Assessment for the Second Classification 27

Table 4: Accuracy Assessment for the Third Classification 31

Table 5: Accuracy Assessment for all Classifications 31

Table 6: Area Covered by Change Classes 40

List of Acronyms

Digital Elevation Model (DEM)

Enhanced Thematic Mapper (ETM)

Enhanced Thematic Mapper Plus (ETM+)

Great Green Wall (GGW)

Great Green Wall for the Sahara and Sahel Initiative (GGWSSI)

Ground Control Points (GCP)

Multispectral Scanner (MSS)

Normalized Difference Vegetation Index (NDVI)

Normalized Difference Water Index (NDWI)

Sahara and Sahel Observatory (SSO)

Scan Line Corrector (SLC)

Thematic Mapper (TM)

Three-North Shelter Forest Program (TNSFP)

United Nations Convention to Combat Desertification (UNCCD)

United States Geological Survey Global Visualization Viewer (USGS GloVis)

Universal Transverse Mercator (UTM)

World Geodetic System 1984 (WGS84)

CHAPTER 1: Introduction

1.1 The Sahel

The Sahel is a geographic region that is situated just south of Africa's Sahara Desert. While its definitions may vary, Udvardy's (1975) *"A Classification of the Biogeographical Provinces of the World"* defines the Sahel as two separate zones, East Sahel and West Sahel. Each zone of the world is attributed such status based on its unique physical characteristics. The most generally accepted depiction of the Sahel describes it as a stretch of land approximately 6000 kilometres long, ranging between 400 kilometres wide at its narrowest points and 600 kilometres at its widest (Figure 1). This swath of land has an area of roughly 3 million square kilometres and passes through nearly a dozen nations, from the Atlantic coast of Senegal to Djibouti's shores on the Red Sea (Le Houerou, 1989).

Like the Sahara Desert, with which it shares a northern boundary, the Sahel is an arid region with infrequent rainfalls. What little rain falls in the region is limited to a short wet season that lasts from June to September (Le Houerou, 1989). However, the Sahel's landscape does vary as it acts as a transition zone between the Sahara Desert to the North and the West African Woodland / Savanna to the South (Udvardy, 1975). With variability in rainfall accompanying change in latitude, fauna and flora also begin to transform. Barren rocky outcrops and sandy dunes change to lonely grasslands and sparsely forested depressions. In these southern parts of the Sahel, small numbers of wildlife continue to exist, despite being brought to near extinction by poaching and overhunting (Le Houerou, 1989). However, time has also considerably changed the landscape of the Sahel. Improper land management coupled with climate change's extreme weather events and rising temperatures have led to widespread desertification and the southwards expansion of the

Sahara. A study by Liu & Xue (2020), found that the Sahara had expanded by 8% between 1950 and 2015. The creeping desert has worried residents of the region for decades, crippling their local economies and starving them of supplies. With the Sahelian grasslands being turned to dust over the years, Sub-Saharan nations have watched as their barrier to the Sahara continues to erode. With a pan-African challenge on the horizon, Sahelian and non-Sahelian nations have begun to unite to devise a plan against widespread desertification (UNCCD, 2021a)

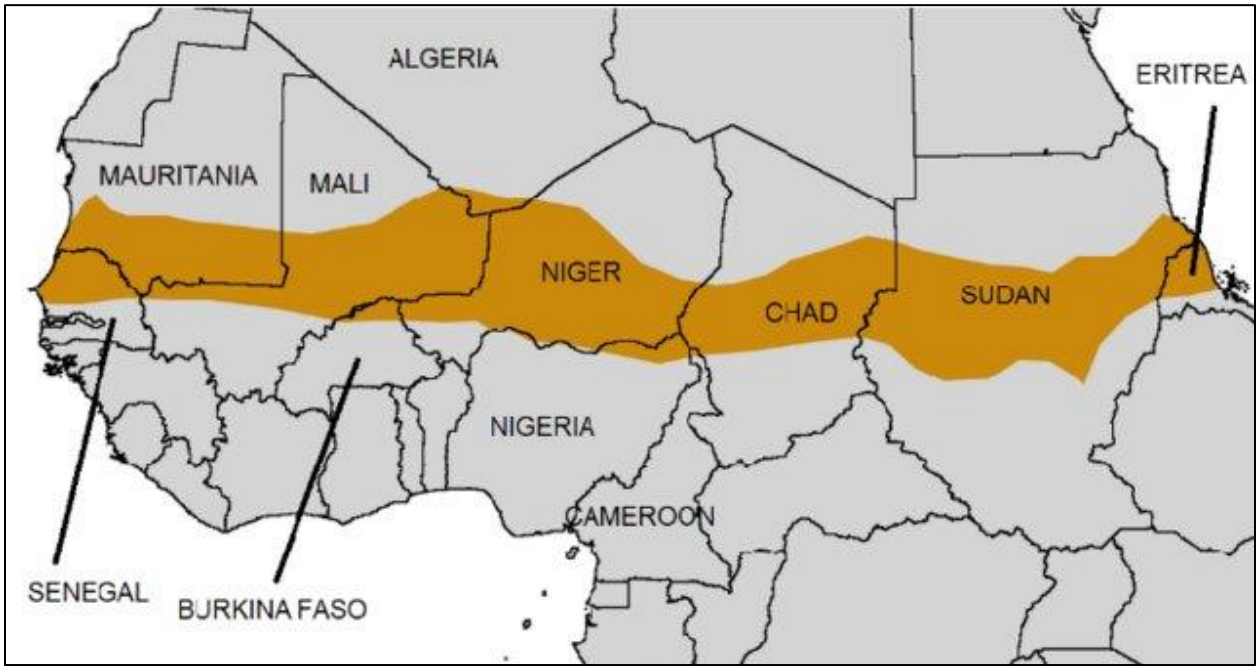

Figure 1: The Sahel Region and it's constituent countries (Doso, 2014).

Today, Sahelian Africa is split into the individual nations of Senegal, Mauritania, Mali, Burkina Faso, Niger, Chad, Sudan and Eritrea. All of these countries became independent in the last century, and most of them have fought through political instability and wars since their autonomy was won or granted. Before colonial powers arrived on the continent, the Sahel was

ruled by kingdoms of indigenous people who warred between themselves, vying for power. However, everything changed as the Partition of Africa began in the late 19th century when European powers burst onto the continent in an effort to expand their empires (McFarland & Rupley, 1998). In many cases, the true intentions of colonial powers were veiled as protectorates and treaties. However, these promises were often short-lived. Soon enough, the native populations of Sahelian Africa, as with other native peoples in Africa, the Americas and Asia, were suppressed by their colonial rulers. In 1914, the world turned into an international battlefield, and many European empires recruited troops from their foreign holdings (McFarland & Rupley, 1998). In a moment of perceived weakness on the French empire's behalf, tens of thousands of villagers from across French West Africa rallied together against their rulers, resulting in the Volta-Bani War. While the movement was stifled within two years, the people of the Sahel had inflicted a noticeable blow. Despite their crucial involvement in the Great War and the Second World War, and even the Indochina war and Algerian war, autonomy was kept away from the people of the Sahel. Only in the 50s and 60s was self-government, and subsequently, independence finally offered to the Sahelian people (Harsch, 2017).

While many countries could now govern themselves, the following historical era was not one of peace and overwhelming success. While nations sought to find a new identity, prospective leaders fought for power, each with their own ambitions and motivations. In Burkina Faso, famed leader Thomas Sankara came to power via the 1983 coup d'état and brought with him a wave of change. A product of Marxist-Leninist ideology, Sankara implemented progressive and anti-imperialist policies such as vaccination efforts, anti-desertification projects, the abolition of polygamy and forced marriages, and literacy campaigns (Harsch, 2014). Despite the humanitarian goals of their new leader, a later coup brought and end to Sankara and his politics. His anti-

imperialist views had earned him criticism, with his successor citing deteriorating international relations as the reason for his takeover (Skinner, 1988).

The story of Burkina Faso's political instability was in no way unique, and to this day, Sahelian nations are plagued with corruption, economic hardship, food insecurity, and war. In a recent study of armed conflicts in the Sahara-Sahel, Brito et al. (2013) claim that "there is now an unprecedented growth in regional instability, characterized by extremist groups carrying out attacks, kidnapping, enslaving, and smuggling arms and drugs to finance their activities". Groups such as Boko Haram and Al-Qaeda have effectively stunted progressive change across the region through their reigns of terror. In a vicious cycle, extremist groups such as the aforementioned ones have preyed upon and recruited those suffering poor living conditions that are only continued through their actions. Furthermore, the violence in the region has made it near impossible for humanitarian organizations to work efficiently and in a secure manner. One such humanitarian project which has been severely affected by the sum of decades of instability is the building of the Great Green Wall (GGW).

1.2 The Great Green Wall

The concept of a Great Green Wall across the Sahel is anything but recent. In 1952, English forester turned environmentalist, Richard St. Barbe Baker, began an ecologically minded expedition into the Sahara. From this adventure into the desert, the Englishman noted the stability provided by tree roots in the Sahel's crumbling soil. Having knowledge of the Sahara's slow expansion, Baker conceived the idea of a vegetation barrier, dubbed the Green Front. While nothing would immediately come from Baker's concept, focus on desertification in the region did begin to increase (Baker, 1989).

Smaller-scale projects combatting desertification, however, would take place before the end of the century, setting the foundations for greater ambitions. For example, Burkina Faso's Thomas Sankara saw the effects of desertification and climate change on his people and took action in the 1980s. He envisioned a wall of 10 million trees to combat the encroaching Sahara, but for his ambitious views, his life was cut short, replaced by a man far less interested in environmental concerns (Leshoele, 2017). Through the late 20th century, desertification became more rampant across the Sahel, mostly unchecked by nations plagued with other issues or simply uninterested in the problem.

It was only in 2005 that then President of Nigeria, Olusegun Obasanjo, revived the idea of a Green Wall across the Sahel. With support from other Sahelian nations, Obasanjo took the prospective project to the African Union, which approved the plan in 2006 (Berrahmouni et al., 2014; Reenberg, 2012). In 2009, a Plan of Action was formally adopted by the African Union, and the following year, the Great Green Wall Agency was created, receiving signatures from all 11 official Sahelian countries (Burkina Faso, Chad, Djibouti, Eritrea, Ethiopia, Mali, Mauritania, Niger, Nigeria, Senegal and Sudan). Along with support from the United Nations Convention to Combat Desertification (UNCCD) and the Global Environment Facility, the new pan-African organization began the Great Green Wall for the Sahara and Sahel Initiative (GGWSSI), the most concrete inception of the green barrier so far (Gadzama, 2017; Reenberg, 2012). In this modernized approach to the decade-old problem, leaders within the organization did not only want to target desertification's environmental impacts but also its social and economic ones. Through the building of the wall, jobs would be created across the subcontinent; sustainable agricultural practices would be encouraged and provide sustenance, all on top of the tangible environmental benefits felt from building the barrier (UNCCD, 2021).

While the concept of the Great Green Wall seems to be incredibly ambitious, similar projects on a smaller scale have achieved varied success in the past. On the African continent, noteworthy examples of greenbelts, green dams or green walls exist in a host of countries. In Morocco, "the biological fixation of coastal dunes along the Atlantic Ocean coast to protect cities such as Tangiers, Kenitra and Agadi" have occurred as early as 1915 (SSO, 2008). In Algeria, a 1500 km long Green Dam was planned in 1971 to combat desertification. While the project initially called for the planting en mass of Aleppo pine, the plan evolved over the decades, eventually turning into an immense infrastructure and agricultural endeavour. While the Algerian Green Dam had numerous shortcomings, many of these can be attributed to poor planning and practices, all of which have been fervently studied since (Goffner et al., 2019). Outside of the African continent, major afforestation projects have also had major impacts. In China, 34.7% of the land area has seen some level of afforestation. A large part of these environmental efforts was contributed to by the Three-North Shelter Forest Program (TNSFP), which began in 1978. This project, which was conducted in northern China's arid and semi-arid lands, covered over 3,300,000,000 square kilometres. Like in Sahelian Africa, this project was targeting desertification and climate change. While much of this area was afforested via traditional tree planting, large swaths were also covered through fruit tree planting, helping residents in an economic fashion (Cao et al., 2020).

While most of these projects had some measurable success, many received criticism. Often, these critiques are tied to the unique circumstances of a project. While reproach may follow a certain narrative for the Chinese Green Wall, they may be completely different for one in the Sahel. With these projects varying broadly in their timeline, expectations and goals may also be completely different. A project deemed doomed to fail in the 1950s may be simpler today, given technological advancements and more advanced knowledge. A common worry with regards to

reforestation projects is that they are too ambitious and thus will either fall short of their intended goal or will be poorly implemented. The Sahara and Sahel Observatory's report (SSO, 2008) on the matter highlights both of these problems as:

> 1) "the 'candidate areas for revitalization' are almost always quite large. Rehabilitating these areas, even slightly, would require enormous resources that the African countries cannot mobilise because of other preceding priorities. In a difficult financial situation, the most adequate strategy is, logically, to concentrate efforts on useful, priority spaces, and eventually, to consolidate or extend these efforts";
>
> 2) "experience has shown that when the quantitative goals are very ambitious, the public authorities tend to outsource the work to a national institution (e.g., the Army for the green dam in Algeria), obscuring the role of the area's communities. This leads to well-known negative effects: jeopardy of sustainability (difficulties with post-investment management) and effectiveness of implementation with technical and logistical problems that make the results rather disappointing, or at least not up to expectations, thus encouraging the planners to lower their aim."

Fifty years after the inception of the Green Dam in Algeria, researchers now know some of the crucial mistakes made that led to some of the dam's shortcomings. These include but are not limited to the monoculture of Aleppo Pine, the total absence of a feasibility study, seed type selection and poor plant transportation as noted in Briki & Khatra (2010), as well as "poor choice of reforestation zones due to extremely limited prior knowledge in terms of biophysical characteristics and climate (environment); ill-adapted nursery protocols, planting densities, plantation dates and poor seed quality (technical), and insufficient staff expertise, and lack of local population buy-in (social)" (Goffner et al., 2019). Post planting procedures such as evaluations

and monitoring were also lacking. In the case of the Three-North Shelter Forest Program, a study from Cao et al., (2020) found that water consumption by vegetation in the green wall was leading to negative impacts. The authors argued that some areas could not sustain prolonged vegetation growth without irrigation, and in others, vegetation was draining groundwater sources. While these specific problems may not plague the Great Green Wall in the Sahel, implementing such a vast idea is evidently very complex. Yet, the UNCCD has already claimed many impressive feats in Sahelian countries like Burkina Faso. In this nation alone, roughly 16 million trees have already been produced, 29602 hectares of land has been restored to pre-desertification conditions, and 26869 people have been trained on food and energy security, amongst many other feats (UNCCD, 2020b).

1.3 Research Objectives

The goal of this study is to gather information regarding the foundations of the Great Green Wall. While opinions on the project today vary from cautious optimism to decisive disbelief, there is not a better indicator of the project's necessity than the landscape itself during periods of pronounced desertification and afforestation. Through the visualization of vegetation change since the 1970s, project stakeholders can possibly be provided information that will contribute towards the project's operation. In addition to quantifying vegetation change directly before and after the implementation of the GGW, the study will seek to understand the ebb and flow of vegetation in the region long before 2005. If understood, these trends can act as a baseline to which post-GGW change can be compared. This goal will be achieved by conducting a change detection analysis utilizing the Landsat satellite program's image archive. By combining land use classifications highlighting vegetation with generic change detection images via a raster calculator, vegetation

growth and loss can be isolated and emphasized on a final map product. The images required for these analyses will be acquired via two separate streams:

1) In the first stream, the Normalized Vegetation Difference Index (NDVI) will be applied to the chosen pair of images; then, the newer images pixel values will be subtracted from the older one. The resulting image will show positive and negative change in the image between the two image dates.
2) In the second stream, a suite of tools (such as spectral indices) will be tested to yield the best possible classification of the study area. This classification will break down the image into broad land use classes, but most importantly, it will be used to highlight vegetation. The accuracy of each tool or combination of tools will be determined via a standardized accuracy assessment tool.

1.4 Study Area

Although the Great Green Wall is set to span the entire African continent, a project detailing it in its entirety would be an arduous undertaking. For this reason, this study will focus on a particular country along the wall's path. Burkina Faso's Sahel region is a perfect test site, as the Great Green Wall will only be implemented in this region. The country's southern regions are considerably lusher with vegetation, placing them in an entirely different geographic region. The study area, however, embodies many of the characteristics of its namesake. All of its 36,737 square kilometres are covered in a flat, arid landscape dotted with lonely acacia trees and dry riverbeds (INSD, 2019). Bodies of water, such as the Mare d'Oursi and the Feildegasse River, appear across the region, but most are incredibly shallow and nearly disappear by the end of the dry season. Most of the thicker vegetation concentrates along creeks or small rivers that come and go depending on rainfall.

The Sahel region is the northernmost of Burkina Faso's 13 administrative regions. It is composed of four provinces, Oudalan, Séno, Soum and Yagha (Figure 2), and despite its relatively small population of 1,395,109 residents, it makes up 6.9% of the national population. While the region, like other Sahelian ones, has experienced constant conflict and difficulties, resulting in outmigration, it has more than doubled its population since 1985 (INSD, 2019). These struggles are well reflected in Burkina Faso's regional poverty and accessibility metrics. In metrics such as proximity to schools, health centres and markets, or access to electricity, transportation, or a refrigerator, it ranks last or second to last (INSD, 2019). Residents who have remained through the turmoil either reside in small remote communities connected solely by makeshift roads or slightly larger towns, such as the capital, Dori. With much of the region's land not suitable for farming, only certain crops can be grown. Despite this, 80% of the population works in the industry. With such difficulties, the success of a massive project like the Great Green Wall could save the Sahel region's inhabitants, and its failure could mean further devastation.

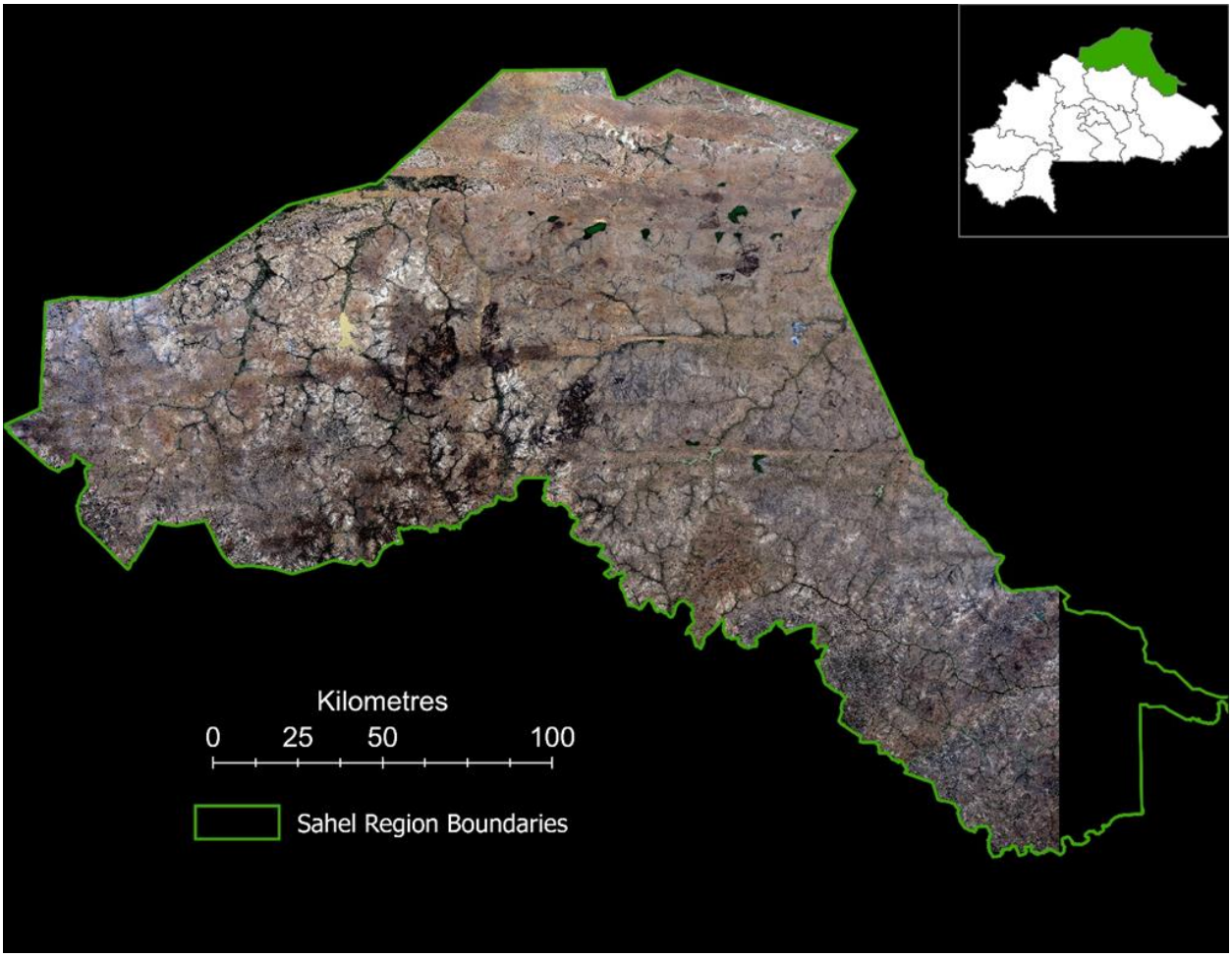

Figure 2: The study area in true colour imaged by Landsat 8, contrasted with the Sahel Region's full boundaries, and the region's location within Burkina Faso (inset map).

CHAPTER 2: Data

2.1 The Landsat program

All raster images for this study were acquired from the United States Geological Survey's Global Visualization Viewer (USGS GloVis) portal. The initial goal was to study images from the Landsat program's inception in 1972 and thus to use images from each of the satellites throughout the program. One of the Landsat program's greatest features is the deep archive of images which spans nearly fifty years. Over this period, NASA and the USGS have launched eight satellites in the Landsat program with progressively superior payloads. Despite the immense catalogue of images available from these satellites, gaps in image quality and availability do exist.

During the program's lifetime, two noteworthy problems have occurred, the launch failure of Landsat 6 and the Scan-Line Corrector failure of Landsat 7. When Landsat 6 launched on October 5th, 1993, it presented two major benefits. Firstly, it would replace Landsat 5, which had already outlived its expected three-year design life. Secondly, the new satellite was equipped with the Enhanced Thematic Mapper (ETM), an improved version of the Thematic Mapper (TM) found on the two previous satellites in the program. Among the improvements brought with the ETM was the inclusion of a new 15-metre resolution panchromatic band (Sheffner, 1994; Markham et al., 2004). Not only would this band offer high resolution black and white imagery, but it could also be used in a process known as Pansharpening, to upgrade the resolution of other bands. Unfortunately, Landsat 6 would never reach orbit during its launch, resulting in a major setback for NASA and the USGS. Landsat 5 would now have to bridge the gap with a less advanced payload until another satellite could be assembled and launched, all while being far beyond its own life expectancy (Sheffner, 1994). The launch of Landsat 7 on April 15, 1999, alleviated these problems temporarily, easing pressure on the 1980's era spacecraft. The newest iteration in the

Landsat program carried the Enhanced Thematic Mapper Plus (ETM+), an improvement on the sensor carried by its ill-fated predecessor. However, misfortune struck again in 2003, four short years after its launch and one year short of its own life expectancy. The scan line corrector (SLC), a component in the ETM+ responsible for the sensor's tracking, failed. This malfunction resulted in missing data gaps across every image obtained since the incident, totalling 22% data loss per image (Markham et al., 2004; Jia et al., 2014). While the resulting images can still be used for certain purposes, Landsat 5 was once again the solution for those requiring complete images. Due to this series of unfortunate events, imagery quality and accessibility have fallen short of their potential for the last two decades. The higher resolution 15-metre spatial resolution images were only available between 1999 and 2003, then again after 2013, whereas they could have been consistently available since 1993 (Landsat 6).

The image selection process also required images to be cloud-free, available within a certain season and processed in a uniform fashion, further limiting image choice. While Landsat satellites have been actively imaging the Earth since 1972, precise locations on the Earth are imaged at different rates based on their orbit. Landsat 7, for example, orbits the Earth in 99 minutes, meaning it can image the rest of the Earth and return to the same place in 16 days (Jia et al., 2014). Landsats 1 through 3 had an orbit roughly 200 km higher (917km rather than 705km), and thus their repeat cycle was 18 days. While spacecraft were calibrated in such a way to "cross the equator on each pass at a time that provides the maximum illumination with minimum water vapour," ideal imaging conditions are impossible to guarantee (Lindgren, 1985; Jia et al., 2014). So while unlikely, it is possible to have infinite periods of minimal visibility in any given area. Another important factor that influences the selection process is the importance of seasonal variability. Consistency in the time of year an image is obtained can sometimes be crucial for

change detection analyses. With seasonal natural events such as snowfall or vegetation growth, it is vital that comparisons are only made between images taken from roughly the same time in the year, at a specific time of the year. Since the wet season in the Sahel region lasts from June to October, images must be acquired after vegetation has started to grow but before it begins to dry out or die (Wu et al., 2020). As such, all the source images for this study were obtained from late September until mid-November. The final major limitation in image availability was the level of preprocessing applied by the USGS before release to the public. In the 28 images obtained for the purpose of this study, all but one image were processed at the "Precision and Terrain Correction (L1TP)" level, while the exception image was corrected to the "Systematic Correction (L1GS) level. From the USGS's processing description website (2021a), we know that:

- "All Landsat scenes are attempted to process to L1TP, using Ground Control Points (GCPs) and a digital elevation model (DEM). In some cases (and more likely in older Landsat data), scene and/or sensor issues, or insufficient reference data can cause L1TP processing to fail. Scene issues include snow, ice, and clouds, which prevent an accurate registration of GCPs within a scene. Sensor issues include measurement/outliers in the spacecraft or instrument telemetry of an interval which also affect the usability of the GCPs. At these times, a L1GT or a L1GS product will be created instead."

Many of the aforementioned problems ultimately led to the omission of images from the study. While the initial goal of the study was to focus on vegetation growth in the Sahel Region since the Landsat's beginning in 1972, this was not achievable. Based on preliminary criteria such as cloud coverage and seasonality, 28 images were initially selected (Table 1). Three images were chosen for each year in six-year intervals, beginning in 1972, the year Landsat 1 was sent into orbit and ending in 2020. With this time period, fluctuations in vegetation growth and loss could be

evaluated for over 30 years, establishing a benchmark to which change after the Great Green Wall could be compared. However, image previews hid the presence of obstructive artifacts in Multispectral Scanner (MSS) images from Landsat 1, 2 and 3 for years 1972 and 1978. Large clouds were also hidden in previews for one of the images from 1984, leading to the removal of that year's images.

Due to the distortion found in the 1978 images, they were also omitted, leaving the 1990 images as the new starting point for the study. Inexplicably, a large gap in image availability was present from 1996 to 1998, leading to the omission of this year in the study as well. This major loss in data, and the resulting effect on the study length, would severely hamper efforts to evaluate pre-GGW vegetation change. The four remaining datasets, 2002, 2007, 2014 and 2020, did not suffer from image unavailability. However, due to Landsat 7's SLC failure in 2003, Landsat 5 images were necessary for 2007. Since the final images were captured by three different satellites using three different sensors, small differences are present in the images. The nine images captured by the Landsat 5 Thematic Mapper all have a spatial resolution of 30 metres and across six spectral bands ranging from 0.45 to 12.5 micrometres. The three Landsat 7 ETM+ images also all have a resolution of 30 metres for the visible light and infrared bands, but additionally have the additional 15-metre panchromatic band. Since this sensor is simply an upgraded version of the original Thematic Mapper, the bands cover the same spectral range, and the image swath is nearly identical. While Landsat 8's Operational Land Imager does not carry the same naming convention as its predecessors, its first four bands share roughly the same specifications as those of the ETM+ (Roy et al., 2014). Only the RED, GREEN, BLUE and NIR bands were retained for each image across all three Landsats, as these bands would be the only ones used. The similarities in sensor and image characteristics are evidence of the benefits of continuity in the Landsat program.

Table 1: All the source images, including those that were omitted (red) and those which were used (green)

Name	Month	Day	Year	Details / Notes
LM01_L1TP_210050_19731003_20180428_01_T2	Nov	13	1972	Omitted due to obstructive artifacts
LM01_L1TP_209050_19721025_20180429_01_T2	Oct	25	1972	
LM01_L1TP_208051_19721024_20180429_01_T2	Oct	24	1972	
LM03_L1GS_210050_19781224_20180421_01_T2	Dec	24	1978	Omitted due to obstructive artifacts and non-uniform preprocessing
LM03_L1TP_209050_19781223_20180421_01_T2	Dec	23	1978	
LM02_L1TP_208051_19780914_20180421_01_T2	Sep	14	1978	
LT05_L1TP_195050_19841112_20170220_01_T1	Nov	12	1984	Omitted due to obstructive cloud coverage
LT05_L1TP_194050_19841121_20170220_01_T1	Nov	21	1984	
LT05_L1TP_194051_19841121_20170219_01_T1	Nov	21	1984	
LT05_L1TP_195050_19901113_20170128_01_T1	Nov	13	1990	Landsat 5 Thematic Mapper
LT05_L1TP_194050_19901122_20170128_01_T1	Nov	22	1990	
LT05_L1TP_194051_19901122_20170128_01_T1	Nov	22	1990	
N/A				No Data Available within Season for 1996 -1998
LE07_L1TP_195050_20021021_20170129_01_T1	Oct	21	2002	Landsat 7 Enhanced Thematic Mapper+
LE07_L1TP_194050_20021014_20170127_01_T1	Oct	14	2002	
LE07_L1TP_194051_20021115_20170128_01_T1	Nov	15	2002	
LT05_L1TP_195050_20070925_20161111_01_T1	Sep	25	2007	Landsat 5 Thematic Mapper
LT05_L1TP_194050_20071004_20161110_01_T1	Oct	4	2007	
LT05_L1TP_194051_20071004_20161112_01_T1	Oct	4	2007	
LC08_L1TP_195050_20141115_20170417_01_T1	Nov	15	2014	Landsat 8 Operational Land Imager
LC08_L1TP_194050_20141108_20170417_01_T1	Nov	8	2014	
LC08_L1TP_194051_20141108_20170417_01_T1	Nov	8	2014	
LC08_L1TP_195050_20201115_20201209_01_T1	Nov	15	2020	Landsat 8 Operational Land Imager
LO08_L1TP_194050_20201108_20201120_01_T1	Nov	8	2020	
LO08_L1TP_194051_20201108_20201120_01_T1	Nov	8	2020	

2.2 Preprocessing

Preprocessing refers to the modification of source data with the goal of preparing it for later analysis. The following practices were performed to make the analysis simpler operationally, less computationally challenging and as accurate as possible. The first tool, Pansharpening, is invaluable to achieve the most precise classification and change detection analysis. This process is only possible if the sensor which captured the image is equipped with a panchromatic band of higher resolution than the other bands. With a panchromatic band included for Landsat 7 and 8 images, exactly half the images were suitable for Pansharpening. Using the tool in PCI Geomatica, all nine images had their spatial resolution improved from 30 metres to 15 metres. While the new resolution still does not allow for the observation of more minor features such as individual trees, it helps with the contouring of larger features such as large buildings, fields, and water bodies, thus increasing the accuracy of classifications.

To conduct the analysis in the most concise fashion, the source images must be arranged into mosaics for each of the interval years. Mosaicking is essential if the goal of the study is to analyze each of the source images together as one study area, and not smaller individual areas. One large advantage to using Landsat imagery is that despite the program's large archive of images, most images are provided in the same location structure, using path and row identifiers. Through the nearly 40 years of images used for this study, three images could be used in each mosaic, all of which are in approximately the same position. Since images within a mosaic were not always captured on the same day, minor atmospheric differences existed between images. However, these inconsistencies were insignificant and therefore did not warrant atmospheric correction. One image covered the majority of the region's western area, another covered the majority of the eastern area, and a final image captured the region's southeastern extremity. While

the use of three images slightly cuts off the region's small eastern panhandle (as seen in Figure 2), this is acceptable as it makes the image acquisition process notably easier.

The mosaicking tool in PCI Geomatica also allowed for the reprojection of source images into a single projection for the resulting mosaic. Since Burkina Faso is split in half by zones as designated by the Universal Transverse Mercator projection, images of the western part of the country were in a different zone (30N) than those in the eastern part (31N). As such WGS84 UTM Zone 30N was chosen across all mosaics to keep consistency.

The final step of preprocessing before spatial analysis was the clipping of the mosaics. Clipping or subsetting of an image refers to the action of reducing an image's extent. This can be done to reduce the image size but keep its shape, or the shape of the image can also be reduced to a pre-set geographic area. Since this study is focused on Burkina Faso's Sahel Region, a georeferenced shapefile approximating the region's shape and size was used to subset all six of the mosaics. However, subsetting the images did come with a few drawbacks. Firstly, since the images were provided by three satellites with slightly different imaging paths and image swaths, one of the mosaics included areas of missing data. The inconsistency in image size may later be problematic as change detection requires each pixel in one image to be compared to another. If one image is smaller than another, then the comparison may be flawed or impossible. To solve this issue, images were further clipped to the extent of the smallest of the available source images. While the resulting images no longer matched the actual boundaries of the region, this is an acceptable loss in the pursuit of a more accurate analysis.

CHAPTER 3: Methods

3.1 Image Differencing

This study is based upon a dual-pronged methodology, in which two separate analysis streams are conducted, and the analyses results are combined to create a final change detection image. In the case of this paper, image differencing was used alongside unsupervised classification to observe vegetation growth or loss between each of four time intervals.

Image differencing refers to the process of subtracting or dividing an image's pixel values by those of a coregistered image, with the goal of evaluating change between images. In the resulting image product, each pixel represents an individual change or lack thereof, indicating positive or negative trends across the image. Specific spectral bands or indices can also be used to target changes in different surfaces or land uses. Per the USGS's guide on Landsat 8 Operational Land Imager Data (2021b), the blue band can be used for bathymetric mapping, while the green band can identify peak vegetation, and the red band can discriminate vegetation slopes. While these bands happen to be useful in the identification of particular features, the combination of certain bands can often seek out these same features with additional accuracy. For instance, while it is known that the green, red and near-infrared bands all aid in the highlighting of vegetation, the Normalized Difference Vegetation Index combines the red and near-infrared bands, ((NIR - RED) / (NIR + RED)) to highlight live green vegetation with higher precision. As opposed to the green or red bands, the near-infrared band's unique interaction with the cellular structure of leaves allows it to differentiate green vegetation from other green surfaces such as artificial turf fields (Karnieli, 2010). In preliminary tests, NDVI performed far superior to the other available bands in the observation of vegetation, and as such, it was chosen as the basis of the image differencing (Figure 3). NDVI values range between 1 (usually depicted in white) and -1

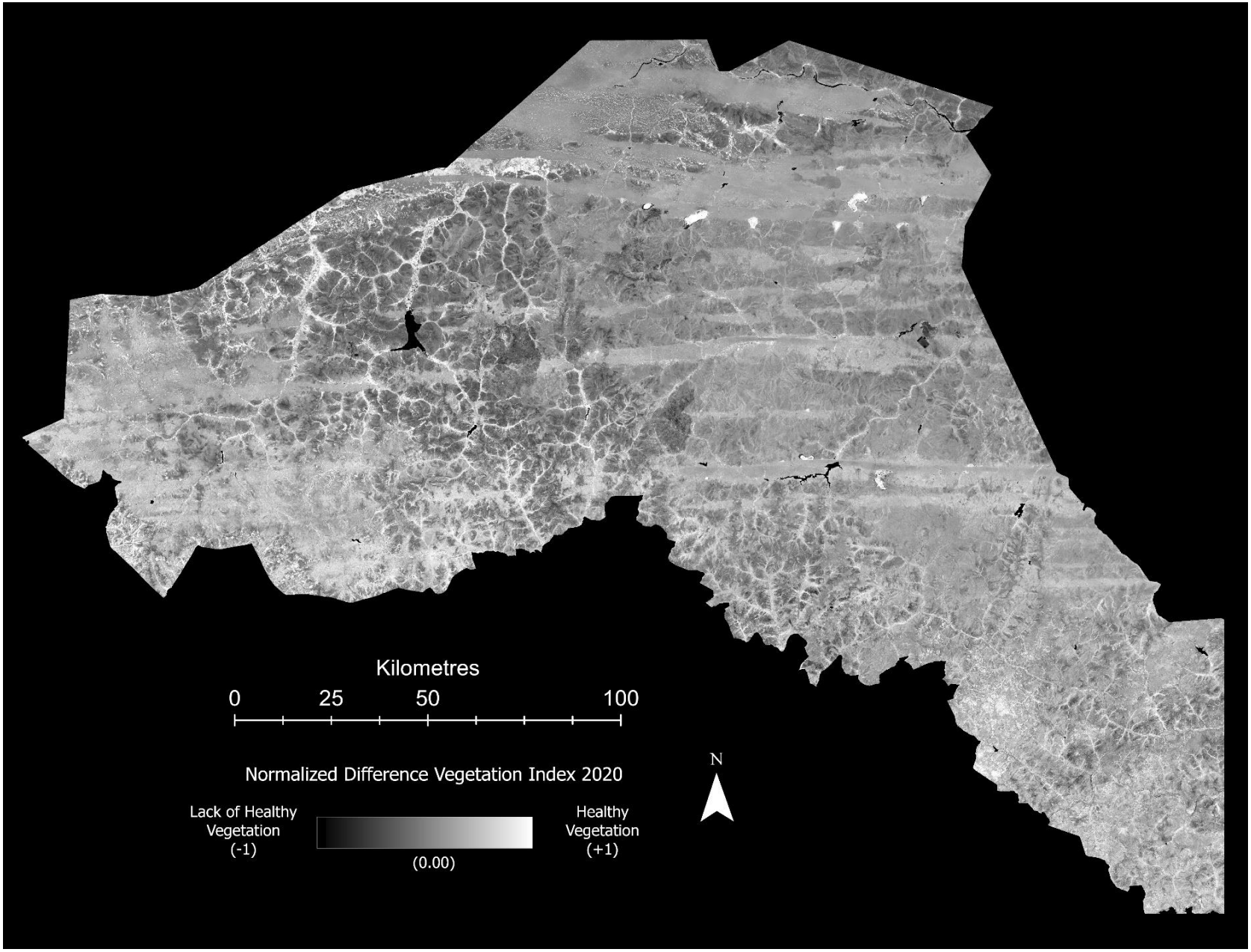

Figure 2: NDVI image of the study area 2020

(usually depicted in black), with higher positive values indicating healthy vegetation and lower negative values indicating a lack of healthy vegetation. Other surface types can also be distinguished based on their NDVI values and general characteristics. Dry soil and rocky areas take on near-neutral index scores, whereas bodies of water are portrayed with strong negative values.

Across each of the four sets of time intervals, pixel values in the earlier images were subtracted by those in the later images (i.e., 1990 minus 2002). In the new image (Figure 4), negative values represented growth, positive values represented loss and pixels with a value of zero represented no change (although these are incredibly rare). As an example illustrating how these results would be obtained, a negative value representing a lack of vegetation minus a positive value representing vegetation would result in another negative value, indicating vegetation growth.

The first class represents general vegetation growth and is occupied by pixel values between (-2) and (-0.01). On the opposite end of the spectrum, the third class represented vegetation loss and is occupied by values between 0.01 and 2. The remaining pixels in the (-0.01) to 0.01 range are composed of no change or meaningless change, and as such, are placed in the second class, aptly named the “No Change” class. All class cut-off values were chosen to limit the size of the no change class, while not rendering it empty, and consequently, purposeless.

3.2 Unsupervised Classification

The second type of analysis conducted was an unsupervised classification to classify land uses within images. Unsupervised classifications differ from supervised classifications as the classification runs itself once the input parameters are set. Conversely, supervised classification requires the creation of training areas that inform artificial intelligence on how features should be classified. This method is also much more difficult without reliable ground-

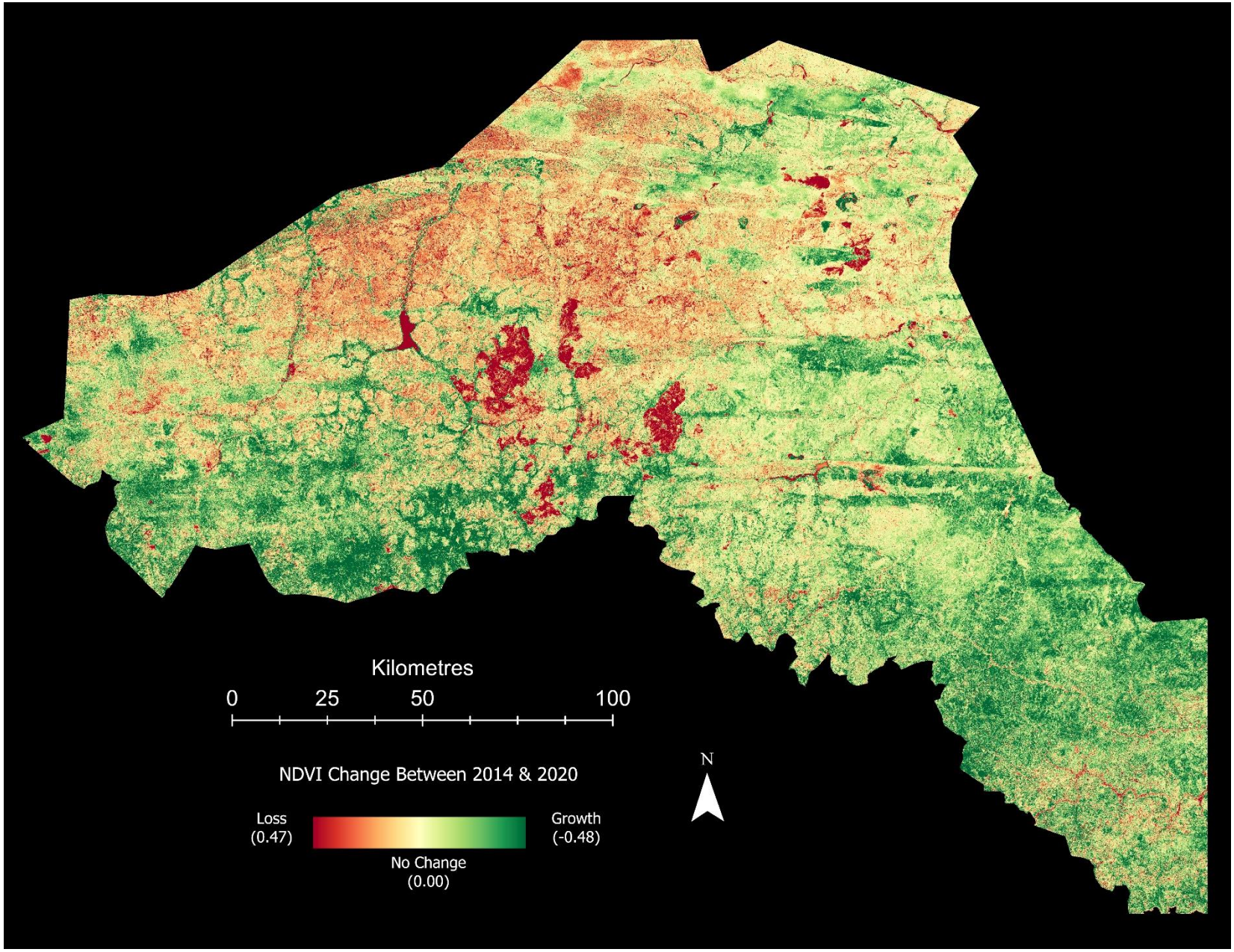

Figure 4: NDVI value change between 2014 and 2020

truthing as poorly chosen training areas can negatively affect the classification's accuracy. The K-Means clustering algorithm, also known as the basic Isodata or migrating means method, seeks to group pixel values into clusters based on the differences between values and the differences between clusters (Duda & Canty, 2002). The classification was set to have 30 output classes and 15 iterations. While a higher number of clusters can generally result in a more discriminating analysis, thus potentially increasing classification accuracy, the classification outputted a dozen or so empty classes each time. These empty classes indicate that the tool could not find any more significant differences between values and classes, and thus no more output classes were required. These classes would then be further classified into five aggregate classes that refer to land uses: Barren land, Vegetation, Water, Built-Up and No Data. The "No Data" class refers to any area outside of the boundaries of the image that was still classified.

In order to choose the best data for classifying images, three rounds of classifications were executed, each with different data inputs, then tested for accuracy. Each successive round of classification would add another layer of data in the hopes of improving upon the preceding classification's results. Accuracy would be measured by generating 200 random points on the image, then comparing the classification of those points to a natural colour reference image to determine whether the area at those points was classified correctly. The most recent mosaic was used as the test data as the higher spatial resolutions could prove useful in the identification of different land uses and geographic features. The first classification was based on the image's visible bands (red, green and blue bands), and as expected, this classification was not very accurate (Figure 5). Both the barren land and vegetation classes were correctly classified in only 66% of cases (Table 2).

Table 2: Accuracy Assessment Results from PCI Geomatica for the first classification

Overall Accuracy: 67.50% - 95% Confidence Interval (60.75% 74.24%) Overall Kappa Statistic: 0.35% – Overall Kappa Variance: -0.03%					
Class Name	**Producer's Accuracy**	**95% Confidence Interval**	**Users Accuracy**	**95% Confidence Interval**	**Kappa Statistic**
Barren Land	66.87%	(59.33% 74.40%)	96.61%	(92.61% 100.31%)	0.8087
Vegetation	66.67%	(48.13% 85.20%)	46.51%	(30.44% 62.58%)	0.3707
Water	0.00%	(-50.00% 50.00%)	0.00%	(-4.16% 4.16%)	-0.0050
Built-Up	0.00%	(0.00% 0.00%)	0.00%	(0.00% 0.00%)	0.0000

Barren land was often misclassified as vegetation or built-up land as its dark brown areas can be confused with vegetation and its grey areas confused with the high reflectance of roof structures (Figure 6). Bodies of water are difficult to identify as all but a few of them in the region take on a light beige silty appearance or a dark green colour due to algal blooms. These unusual appearances, in contrast with the expected blue colour, result in misclassification with the sandy appearance of barren land or terrestrial vegetation. Even the most natural-looking lake in the image, Lake Higa in the southeast corner of the region, was misclassified as vegetation despite its deep blue colour.

In the second classification, the Normalized Difference Vegetation Index (Figure 3) was added to the visible bands (Figure 2) to facilitate the classification of vegetation. Unexpectedly, much of the area covered by the vegetation in the previous classification was now classified as barren land (Figure 6). General accuracy for the classification rose significantly from 67.5% to

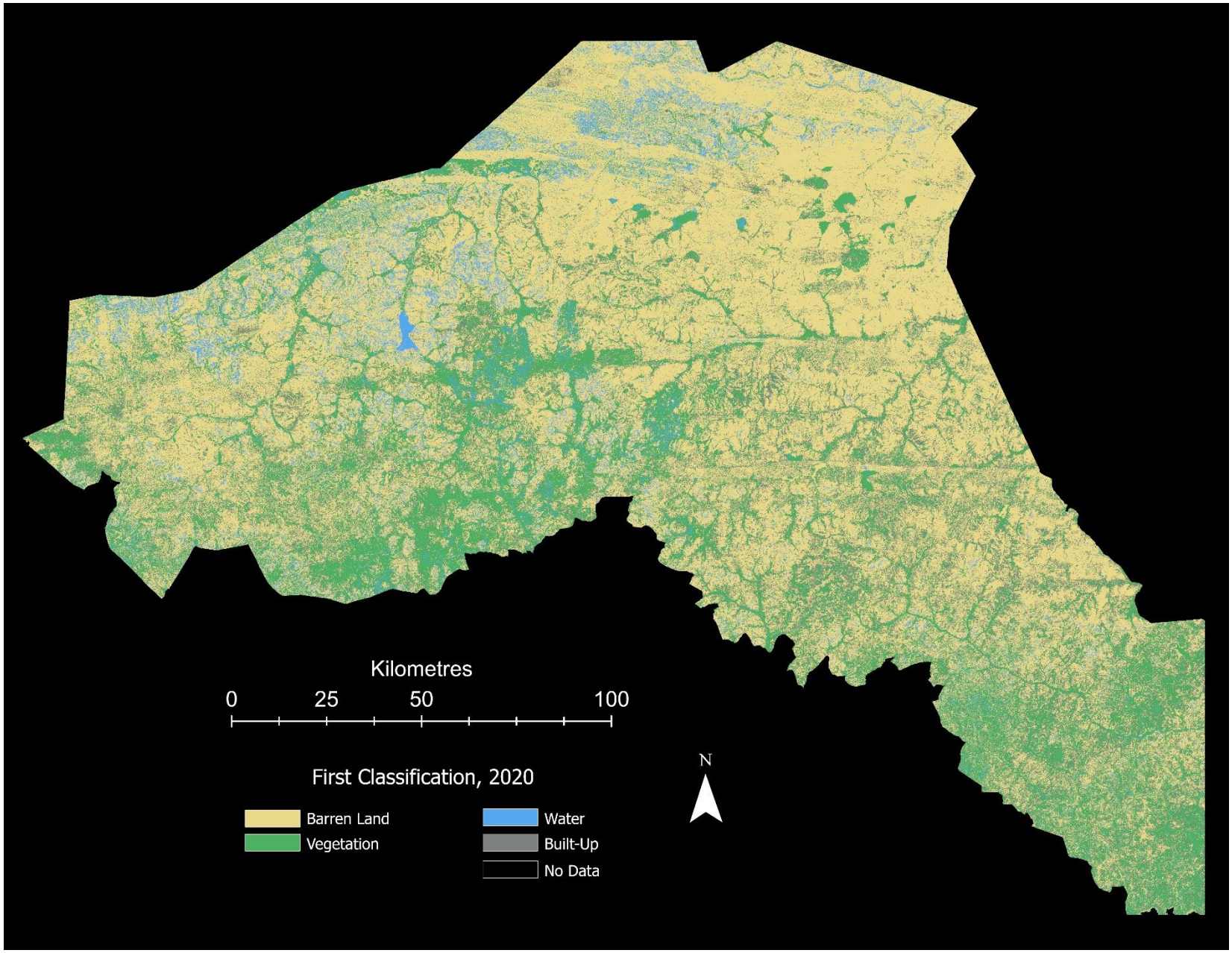

Figure 5: The first classification results

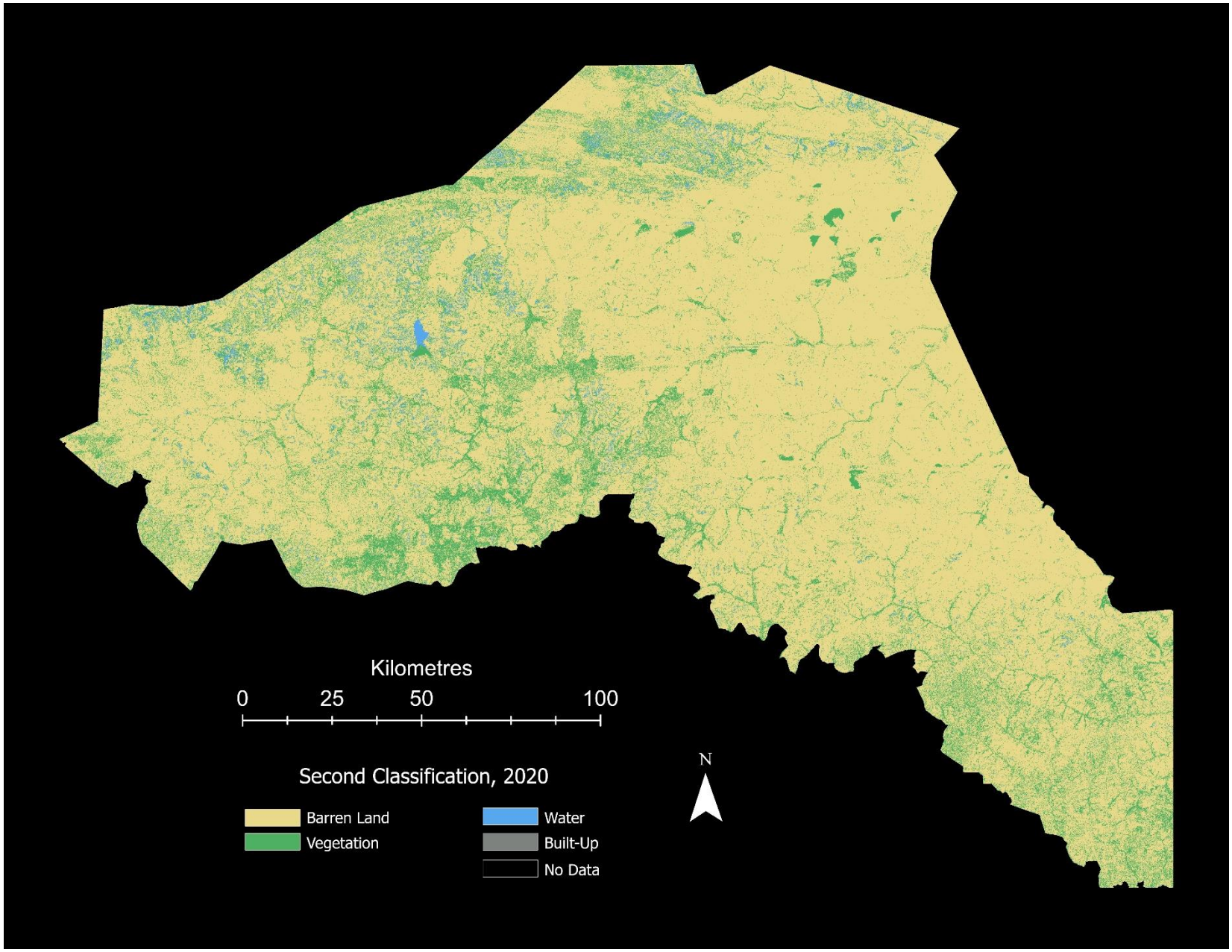

Figure 6: The second classification results

82%, and barren land's accuracy rose to 87.4%, but the vegetation class accuracy plummeted to 45% (Table 3). While the addition of NDVI seemed to fix some previous problems, it invited others. One prominent change in the second iteration of classifications was the lack of output classes aggregated into the built-up class. While the previous classification identified a spectral class in some of the region's population centres, the newest classification did not. As such, misclassification between the barren land class and the built-up class fell dramatically (from 22 misclassifications to 0) due to NDVI's strong ability to inadvertently identify water bodies.

Table 3: Accuracy Assessment Results from PCI Geomatica for the second classification

Overall Accuracy: 82.00% - 95% Confidence Interval (76.42% 87.57%) Overall Kappa Statistic: 0.30% – Overall Kappa Variance: 0.02%					
Class Name	**Producer's Accuracy**	**95% Confidence Interval**	**Users Accuracy**	**95% Confidence Interval**	**Kappa Statistic**
Barren Land	87.42%	(82.23% 92.62%)	92.16%	(87.78% 96.55%)	0.3735
Vegetation	45.00%	(20.69% 69.30%)	30.00%	(11.93% 48.06%)	0.2222
Water	0.00%	(-16.66% 16.66%)	0.00%	(-25.00% 25.00%)	-0.0152
Built-Up	0.00%	(0.00% 0.00%)	0.00%	(0.00% 0.00%)	0.0000

The Normalized Difference Water Index (NDWI) was added to the previous classification's input bands in the third classification in an effort to reduce misclassifications between vegetation and water classes (Figure 7). McFeeters' NDWI (1996) was developed to "delineate open water features and enhance their presence in the remotely-sensed digital imager." Like the NDVI, it is calculated with a simple equation consisting of two bands (GREEN – NIR / GREEN + NIR) While this index was able to distinguish small rivers with high precision, it still struggled with algae-

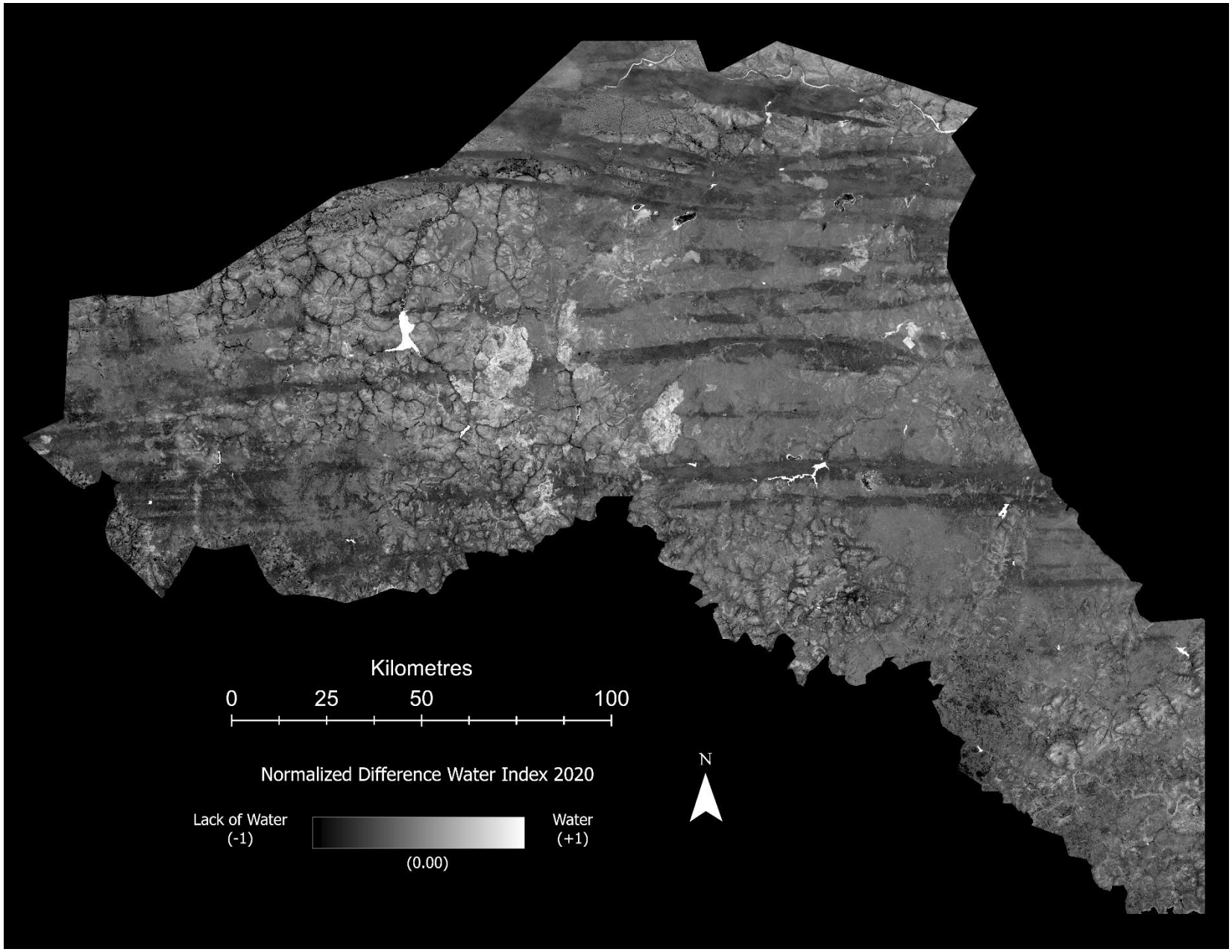

Figure 7: NDWI image of the study area in 2020

covered lakes and ponds (Figure 8). Large swaths of presumably damp land and certain artificial structures also displayed notably high reflectance through the use of the index. Despite the NDWI's inability to classify water bodies with algal blooms as water, the accuracy of the vegetation class rose from the previous classification's 45% to 66.6% (Table 4). While overall accuracy dropped slightly in this third classification, the importance of the vegetation class' accuracy supersedes overall accuracy. This classification was also still more accurate than the first, presenting a clear pick in classification method for the other images (Table 5).

With the 2020 image classified, the third classification methodology was applied for the three remaining mosaics (2002, 2007, 2014). While each time interval was composed of two images, an older one and a more recent one, only one image needed to be classified for each interval. The more recent image was selected for all three of the intervals, as this image represented a more recent depiction of land use. It must also be acknowledged that since the classification accuracy tests were only done using the 2020 mosaic, classification accuracy may vary for other images. This is to say that, had the accuracy testing been done on Landsat 5 or Landsat 7 mosaics, accuracy values may have differed from those obtained from the Landsat 8 mosaic.

Each class was also given a unique identifying number that would be used to combine the image differencing products with the land use classification ones. The three image differencing classes (growth, no change, and loss) were given identifiers from one through three, respectively. The five classification classes (Barren Land, Vegetation, Water, Built-Up, and No Data) were given identifiers that are multiples of ten, from ten to fifty. When the images are added together through the raster calculator, overlapping classes from each image are fused together to create new classes. With the new class comes a unique class identifier produced by the addition of the two previous classes' identifiers. For example, if the growth ID = 1 and the vegetation ID = 20,

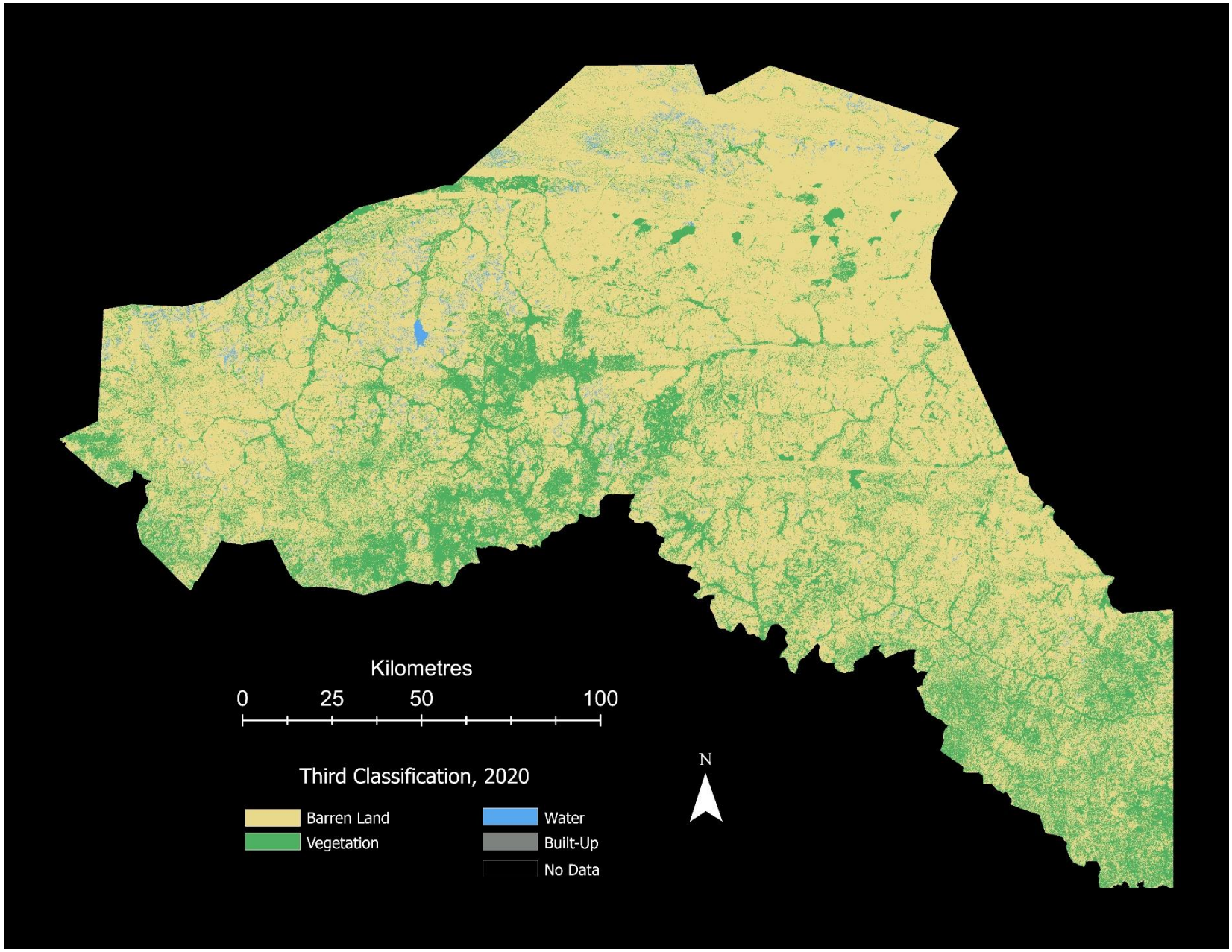

Figure 8: The third classification results

then the vegetation growth ID = 21. Since no other class combinations can sum to 21, this new class is unique and can be easily identified. For the sake of this study, the vegetation growth and the vegetation loss classes will be the only ones of interest for the remainder of the paper.

Table 4: Accuracy Assessment Results from PCI Geomatica for the third classification

Overall Accuracy: 79.50% - 95% Confidence Interval (73.65% 85.34%) Overall Kappa Statistic: 0.45% – Overall Kappa Variance: 0.42%					
Class Name	**Producer's Accuracy**	**95% Confidence Interval**	**Users Accuracy**	**95% Confidence Interval**	**Kappa Statistic**
Barren Land	81.32%	(75.09% 87.55%)	94.40%	(90.28% 98.52%)	0.6709
Vegetation	66.66%	(45.72% 87.61%)	34.04%	(19.43% 48.65%)	0.2502
Water	50.00%	(-44.29% 144.29%)	50.00%	(-44.29% 144.29%)	0.4949
Built-Up	0.00%	(0.00% 0.00%)	0.00%	(0.00% 0.00%)	0.0000

Table 5: Accuracy Assessment Results for all three classifications

Classification	**Barren Land**	**Vegetation**	**Water**	**Built-Up**	**Overall**
1. Visible Bands	66.87%	66.66%	0.00%	0.00%	67.50%
2. 1 + NDVI	87.42%	45.00%	0.00%	0.00%	82.00%
3. 1 + 2 + NDWI	81.32%	66.66%	50.00%	0.00%	79.50%

CHAPTER 4: Results & Discussion

4.1 1990 to 2002

Once the change detection layers were completed, each time interval's two change classes (vegetation growth and loss) were combined with the more recent natural colour image. The latter is the same image used to create the land use classification for the respective time interval. The natural colour image helps in the detection of underlying geographic features, as well as areas that have not sustained change during the image's time interval. All vegetation growth and loss, as previously defined, were tracked in green and red, respectively. The bold contrast between layers allows the analyst to identify the location of changes and any relevant patterns it may display in relation to the landscape below. Pixel counts for both of the image's classes were also generated when the new change detection images are created. By combining these counts with the image's respective pixel size (or spatial resolution), the classes' coverage area can be calculated and thus compared over different periods.

The 1990 to 2002 analysis revealed massive vegetation loss across the entire Sahel region (Figure 9). Over 9608.75 square kilometres of the region's area experienced a reduction in vegetation between these two years. This loss contrasts heavily with the quite low 373.02 square kilometres that experienced vegetation growth. Furthermore, from the change image, many of the small growth hotspots are located on bodies of water. The most prominent cases of this are the Mare d'Oursi, in the northcentral part of the image or the river network in the southeastern corner of the image. Vegetation loss also covers some major water bodies, such as the unnamed lake next to the village of Gomde, or the Mare de Dori. While these changes perhaps indicate the beginning or end of an algal bloom, they also prove to be a nuisance in quantifying terrestrial vegetation changes. Vegetation loss, however, was not limited to water bodies and expanded into many of the

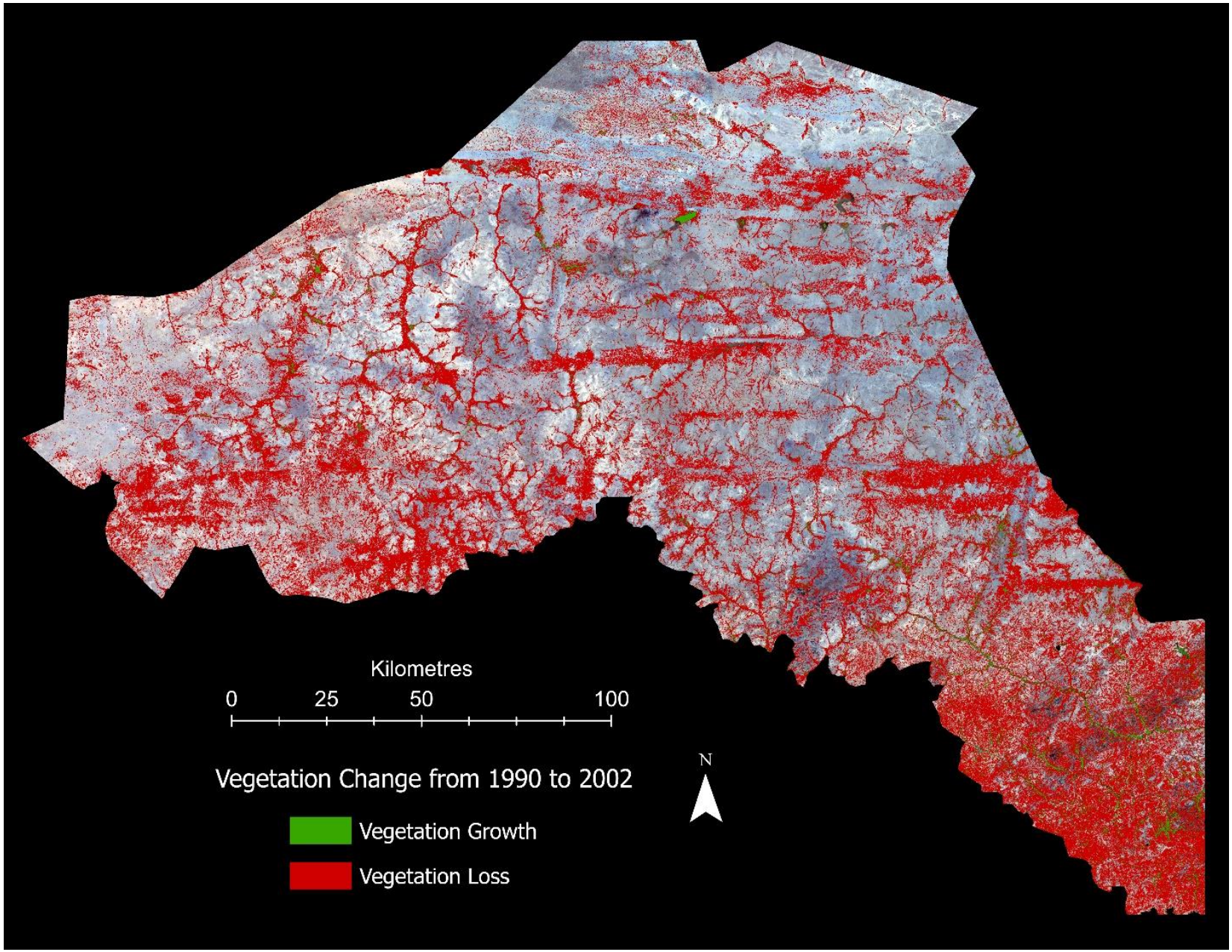

Figure 9: Vegetation Change between 1990 and 2002

study area's valleys, along its rivers and even across its plains. This loss also appeared to be occurring in denser patches along more extreme topography and more sparsely in the plains and other flat areas. The only major exception to this observation is the dense vegetation loss in the southeastern corner of the study area. Here, the dense vegetation loss class covers most of the surface area, with small pockets of growth peeping through along rivers and streams. Other clusters of vegetation loss occurred in longitudinal bands matching underlying geographical formations.

4.2 2002 to 2007

The 2002 to 2007 analysis (Figure 10) resulted in extreme opposite findings to the previous time interval. All prior vegetation loss seems to have been balanced by near-identical vegetation growth in the same places during this time period. However, despite the growth class appearing similar to the previous time interval's loss class, this class's coverage was far denser. Through its pixel count, it was determined that 15357.19 square kilometres had experienced vegetation growth between 2002 and 2007. Additionally, only 4.61 square kilometres had experienced vegetation loss in this time period. This is reinforced by the complete lack of red colouring on the image at first glance. While the image was no perfect mirror image to that of the previous time interval, it showed approximately the same patterns. Though, growth did seem to be slightly sparser in the southwest and denser in the west. Again, most large bodies of water were shown to have grown vegetation as a result of algal blooms or possibly prior misclassifications in the study. Such extreme results as a whole may be a sign of problems in the methodology but could also point towards a trend back to normalcy after extreme climatic conditions in the period between 1990 and 2007.

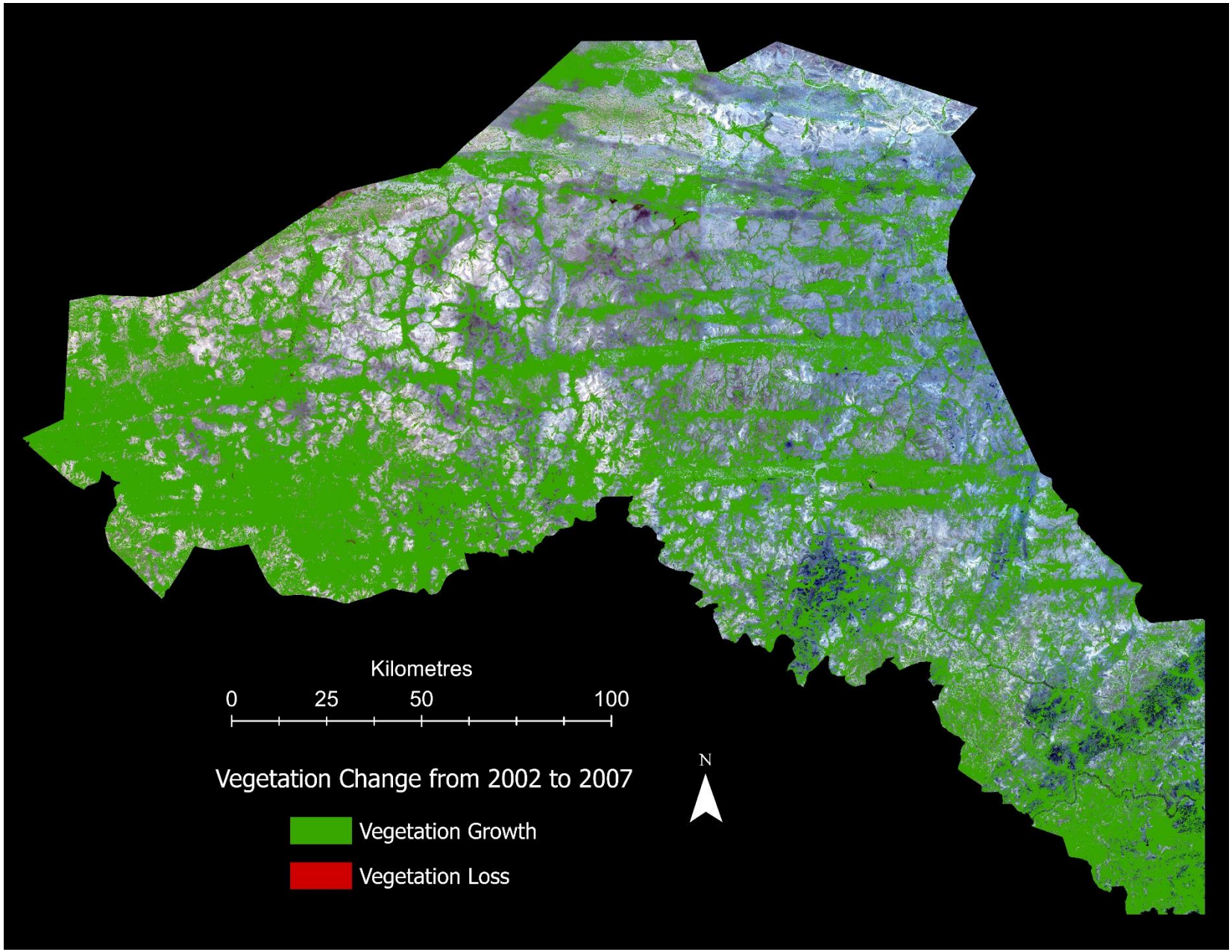

Figure 10: Vegetation Change between 2002 and 2007

4.3 2007 to 2014

The third time interval from this study contributed far less extreme results (Figure 11). A blend of vegetation growth and loss which seemed to be far more even than the two preceding results. Pixel counts from this image indicate that the vegetation growth class occupied 4056.48 square kilometres of the study area, whereas vegetation loss covered 5660.66 square kilometres. While the loss class seems to stick to the same valleys and rivers in a dense uniform fashion as with previous results, the growth class seems to appear far less dense and on the periphery of geographic features. Vegetation growth also appears denser in concentrated pockets across the region, a pattern not yet seen in previous images. This image has also notably classified large water bodies far more accurately, not depicting the lake near Gomde or the Feildegasse River as vegetation at all. Regardless of this, many of the other water bodies, such as the Mare d'Oursi and Mare de Dori, were classified as vegetation loss zones. While this image may be a blow to those hoping for further vegetation growth in the region, the image must also be contextualized by previous findings. With such large-scale vegetation growth between 2002 and 2007, continual vegetation growth may be at its limits. As such, this image may also be a sign of vegetation stabilizing after a massive peak.

4.4 2014 to 2020

The final time interval yielded an image that appeared similar to that of the 2007 to 2014 period at first glance (Figure 12). Vegetation growth now covered 5685.49 square kilometres, handily overtaking vegetation loss, which only covered 1309.98 square kilometres. Similar to the previous image, vegetation growth was not rigidly limited to valleys and rivers, yet the image did show proof of some large clusters of vegetation growth, a pattern not seen previously. Like with the 2007 to 2014 period, the same large bodies of water were also once again not misidentified

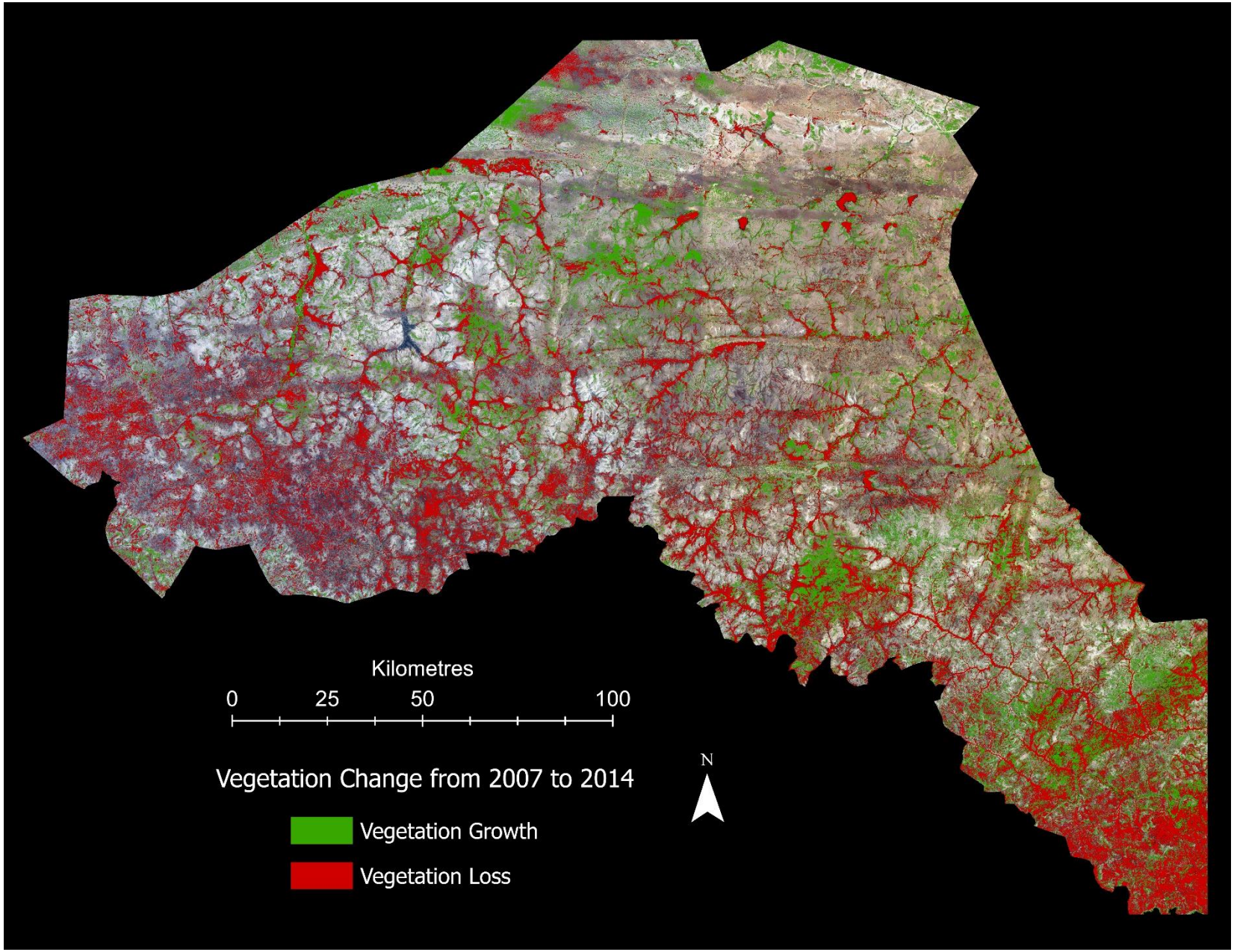

Figure 11: Vegetation Change between 2007 and 2014

However, this final image also possessed several unique qualities. The northern portion of the image saw very little overall change as opposed to all three of the previous change detection images. There were also several large, dense vegetation loss clusters in the centre of the image. These clusters share no similarities with those in the previous image, yet their conspicuous proximity to each other may be telling of some specific event or unified conditions. While documentation indicates that large-scale environmental degradation, including deforestation, fires and overgrazing occurred between 2012 and 2013, no noteworthy vegetation loss event has been specified in the region since 2014 (ACAPS, 2019).

4.5 Implications and Discussion

Despite large changes to the study's temporal scope and partial changes to the physical study area, the findings of this study are intriguing. The extreme nature of changes in vegetation through the 1990s into the 2000s may summon more questions than they answer. The same can be said for the latter half of the timeline, in which change became far more subtle (Table 6). Since the beginning of this research, data availability has been instrumental in analyzing a corner of the world that has long been ignored. Since Landsat satellites were designed to image the entire globe without targeted or prioritized regions, they have allowed time-series analyses into the past for remote regions. The quantification of past changes is possible at a scale not previously attainable. However, the unavailability of qualitative data has made the contextualizing of quantifiable data a far more complex task than initially perceived. Although the results of such a study could lead to conceptual breakthroughs for projects like the Great Green Wall, the observations made are inconclusive without additional contextual information such as local knowledge or insight from other disciplines (i.e., climatology, biology, history). Without additional information, arguments for the continuation of the wall could be made as easily as arguments against it. As seen in Figure

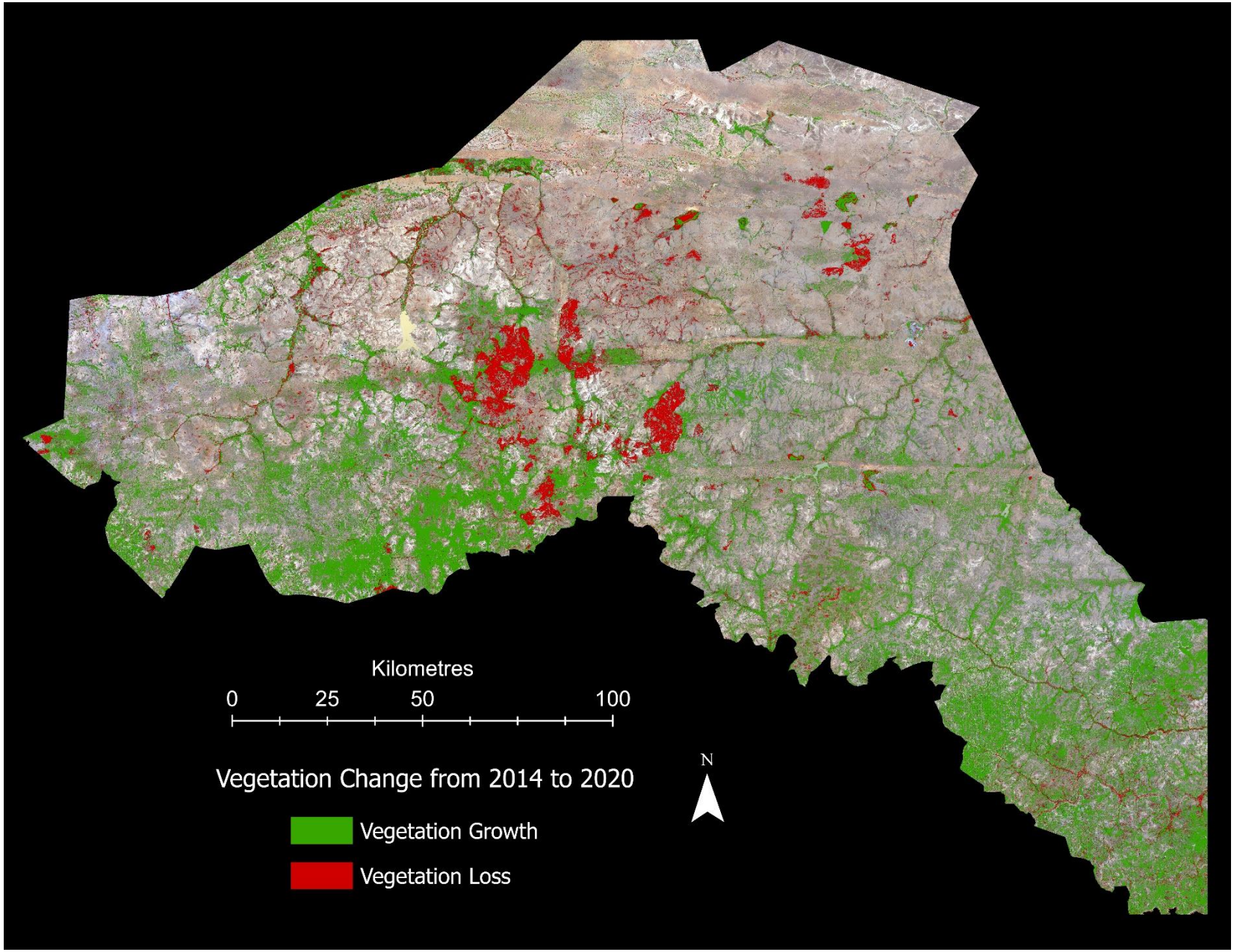

Figure 12: Vegetation Change between 2014 and 2020

13, vegetation growth has fluctuated greatly over the past three decades. Growth outweighed loss for two of the time intervals during or after 2005, and for another, they were almost even. This could indicate a positive trend for the GGWSSI in a battle against all odds. With results such as these, critics should be satisfied and additional funding for the project may be justified. Studies of each individual time interval could also be led to determine what factors are responsible for the higher growth between 2002 – 2007, and 2014 – 2020. However, the quantitative results could also be totally unrelated to the Great Green Wall for the Sahara and Sahel Initiative. These results could be a sign that natural vegetation is growing back

Table 6: Area Covered by Change Classes in Square Kilometres

Time Intervals	**Vegetation Growth**	**Vegetation Loss**	**Net Change**
1990 to 2002	373.02 km^2	9608.75 km^2	-9235.73 km^2
2002 to 2007	15357.19 km^2	4.61 km^2	15352.58 km^2
2007 to 2014	4056.48 km^2	5660.66 km^2	-1604.18 km^2
2014 to 2020	5685.49 km^2	1309.38 km^2	4376.11 km^2

on its own, independently of any afforestation efforts. With additional resources, these trends could be attributed to climatological conditions such as increased rainfall or decreases in heat. In this case, there may be an argument against the continuation of the project, as it has drawn incredible financial resources that could be diverted to other causes. Regardless, of these possibilities, studies on the Great Green Wall, must continue both in Burkina Faso and the rest of the Sahel, as this is the only way to know whether this is the success of the century or it’s largest failure.

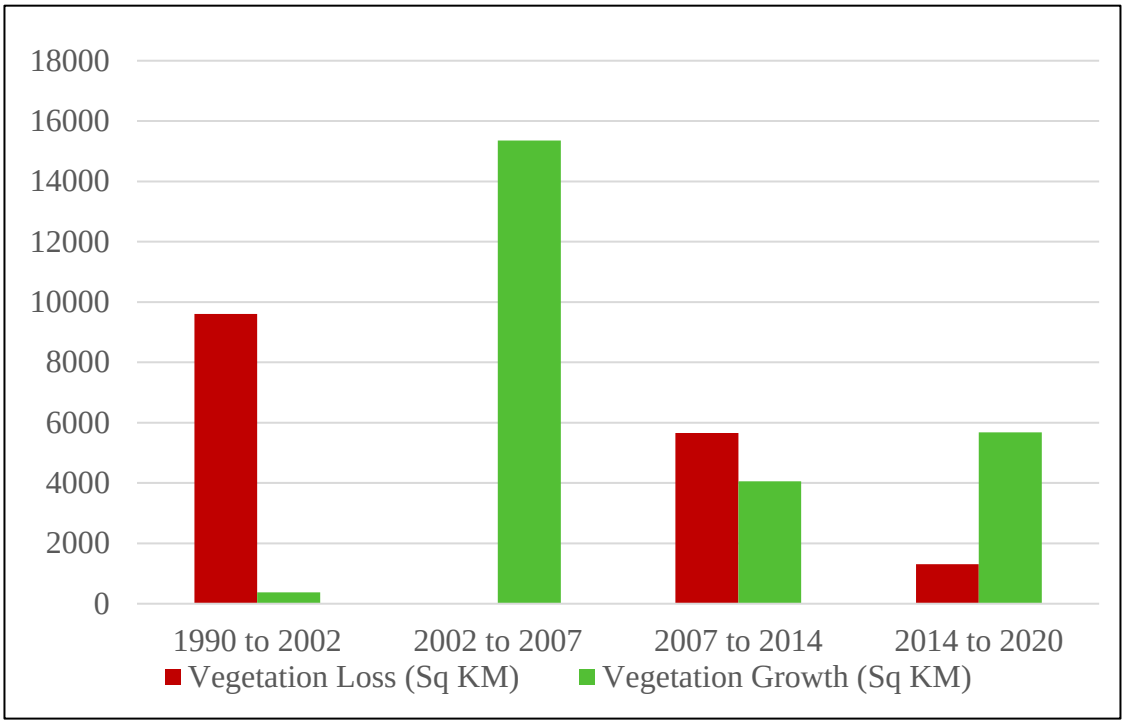

Figure 13: 30 Years of Vegetation Change in Sahel, Burkina Faso

Chapter 5: Conclusion

The Great Green Wall is as unique a project as it is an ambitious one. Thousands of kilometres long, hundreds of kilometres wide, with the livelihood of millions at stake, its success is far from guaranteed. Plagued by logistical problems as much as by violence and corruption, the cause has been doubted by all. However, the fight that it leads is also an essential one. The Sahel is disappearing, crushed by an ever-expanding desert that engulfs the necessities for life in the region and plunges the Sahelian people into further despair. With previous green walls and dams achieving success, the difficulty of a Great Green Wall across the Sahel relates to the project's sheer scope. Through the use of mixed remote sensing methods such as image differencing, spectral indices and unsupervised classification, it appears that vegetation has slowly begun to return to the region. Vegetation growth outpaced vegetation loss in the study area nearly five to one between 2014 and 2020. However, attributing this success to GGW is impossible. A lack of contextual data relating to climatic conditions, individual project advances, and local observations (both current and historically), leads to difficulties in establishing causal relationships between perceived progress and reality. So as the Great Green Wall continues forward, hopefully, this study can provide some of the quantitative information needed to solve such a complex conundrum. Will the Great Green Wall work?

5.1 Limitations

Although this study was hampered by limitations in data since the very beginning, the effects of these constraints could not be foretold until the completion of the analysis. However, with the results now available, the importance of contextual qualitative data is apparent. The immense shift from extreme vegetation loss through the 1990s to the extreme growth of the early 2000s almost appears to be a methodological error given the results. With additional contextual

information such as precipitation data, perhaps these gaps in certainty could be partially filled. The absence of these data is not unsurprising either, given the poor quantity and quality of data produced by Burkina Faso authorities, especially over the last thirty years. While precipitation data for more developed regions of the world were available within the timeframe of this study, a lack of weather instrumentation and reporting in the region created a gap that may never be filled.

It must also be noted that all vegetation change images capture solely the differences between the source images and cannot describe the series of minor changes that may make up a final change. For example, if vegetation grew steadily between 2020 and 2029, a serious drought in 2029 could wipe out any sign of previous vegetation growth and simply show vegetation loss between 2020 and 2030. While the use of smaller time intervals over the same time period could alleviate this issue, it would also require far more time and data. While not perfect, the choice in time intervals was heavily influenced by the lack of data on a finer temporal scale.

One of the foundational components for this project, the large archive of publicly available Landsat data, also quickly became a severe limitation for the scope of this study. Image unavailability from the 1970s through the 1990s due to a wide range of technical problems severely limited the length of the timeline for this analysis. Furthermore, the data that were available are of lower spatial resolution as opposed to newer imaging systems. The 30-metre resolution of Landsat 5 and 15-metre resolution of Landsats 7 and 8 have difficulty identifying sparse vegetation, such as that of the Sahel. Single groups of trees may only be recognized as a grey pixel that averages the dark tones of vegetation with the light tones of the surrounding sand. For future attempts at quantifying vegetation change, it may be best to try and obtain airborne imagery of at least 1-metre resolution. As a result of this unsatisfactory resolution, even the most accurate classification method was mediocre at best, putting into question the usefulness of the final results.

References

ACAPS, (2019). *Burkina Faso: Escalation of Armed Violence. Burkina Faso Escalation of Conflict Briefing Note, November 1st 2019*. Retrieved from: https://www.acaps.org/sites/acaps/files/products/files/20191101_acaps_briefing_note_conflict_in_burkina_faso.pdf

Baker, R. B. (1989). *Man of the Trees: A Centenary Tribute*. Indian National Trust for Art and Cultural Heritage, New Delhi.

Berrahmouni, N., Tapsoba, F., Berte, J.C. (2014). The Great Green Wall for the Sahara and the Sahel Initiative: Building Resilient Landscapes in African Drylands. Pages 15–18. In: Bozzano M, Jalonen R, Thomas E, Boshier D, GalloL, Cavers S, Bordács S, Smith P, Loo J. *Genetic Considerations in Ecosystem Restoration Using Native Tree Species. State of the World's Forest Genetic Resources—Thematic Study*. FAO and Bioversity International,Rome, Italy

Brito, J.C., Godinho, R., Martínez-Freiría, F., Pleguezuelos, J.M., Rebelo, H., Santos, X., Vale, C.G., Velo-Antón, G., Boratyński, Z., Carvalho, S.B., Ferreira, S., Gonçalves, D.V., Silva, T.L., Tarroso, P., Campos, J.C., Leite, J.V., Nogueira, J., Álvares, F., Sillero, N., … Carranza, S. (2014), Unravelling biodiversity, evolution and threats to conservation in the Sahara-Sahel. *Biological Reviews*, 89, 215-231. https://doi.org/10.1111/brv.12049

Cao, S., Suo, X., & Xia, C. (2020). Payoff from Afforestation Under the Three-North Shelter Forest Program. *Journal of Cleaner Production*, 256, 120461. https://doi.org/10.1016/j.jclepro.2020.120461

Doso Jnr, S. (2014). Land degradation and agriculture in the Sahel of Africa: causes, impacts and recommendations. *Journal of Agricultural Science and Applications*, 3, 67-73. 10.14511/jasa.2014.030303

Duda, T., & Canty, M. (2002). Unsupervised Classification of Satellite Imagery: Choosing a Good Algorithm. *International Journal of Remote Sensing*, 23(11), 2193-2212. https://doi.org/10.1080/01431160110078467

Gadzama, N. M. (2017). Attenuation of the Effects of Desertification Through Sustainable Development of Great Green Wall in the Sahel of Africa. *World Journal of Science, Technology and Sustainable Development*, 14(4), 279-289. https://doi.org/10.1108/WJSTSD-02-2016-0021

Goffner, D., Sinare, H. & Gordon, L.J. (2019). The Great Green Wall for the Sahara and the Sahel Initiative as an Opportunity to Enhance Resilience in Sahelian Landscapes and Livelihoods. *Regional Environmental Change*, 19, 1417–1428. https://doi.org/10.1007/s10113-019-01481-z

Harsch, E. (2017). *Burkina Faso: A History of Power Protest and Revolution*. Zed Books, Ltd., London.

Harsch, E. (2014). *Thomas Sankara: An African Revolutionary*. Ohio University Press, Athens.

Institut National de la Statistique et de la Démographie (INSD). (2019). *La Région du Sahel en Chiffres*. Retrieved from: https://www.insd.bf/contenu/statistiques_regions/regions_en_chiffres_en_2019/Sahel%20en%20chifre%202019.pdf

Jia, K., Wei, X., Gu, X., Yao, Y., Xie, X., & Li, B. (2014*).* Land Cover Classification Using Landsat 8 Operational Land Imager Data in Beijing, China. *Geocarto International*, 29(8), 941-951. https://doi.org/10.1080/10106049.2014.894586

Karnieli, A., Agam, N., Pinker, R. T., Anderson, M., Imhoff, M. L., Gutman, G. G., Panov, N., & Goldberg, A. (2010). Use of NDVI and Land Surface Temperature for Drought Assessment: Merits and limitations. *Journal of Climate*, 23(3), 618-633. https://doi.org/10.1175/2009JCLI2900.1

Le Houérou, H.N. (1989). The Grazing Land Ecosystems of the African Sahel. *Ecological Studies*, 75. Springer-Verlag, Heidelberg. http://doi.org/10.1007/978-3-642-74457-0

Leshoele, M. (2017). Thomas Sankara's Revolutionary Leadership-Meditations on an African Statesman. *Africa Insight*, 47(2), 40-53.

Lindgren, D. T. (1985). *The Landsat System. In Land Use Planning and Remote Sensing* (pp. 67-86). Springer, Dordrecht.

Liu, Y., & Xue, Y. (2020). Expansion of the Sahara desert and shrinking of frozen land of the Arctic. *Scientific Reports*, 10(1), 4109-4109. https://doi.org/10.1038/s41598-020-61085-0

Markham, B. L., Storey, J. C., Williams, D. L., & Irons, J. R. (2004). Landsat Sensor Performance: History and Current Status. IEEE *Transactions on Geoscience and Remote Sensing*, 42(12), 2691-2694. https://doi.org/10.1109/TGRS.2004.840720

McFarland, D. M. & Rupley, L. A. (1998). *Historical Dictionary of Burkina Faso*. Lanham, MD: The Scarecrow Press.

McFeeters, S. K. (1996). The Use of the Normalized Difference Water Index (NDWI) in the Delineation of Open Water Features. *International Journal of Remote Sensing*, 17(7), 1425-1432. https://doi.org/10.1080/01431169608948714

SSO (2008) *The Great Green Wall Initiative of the Sahara and the Sahel: introductory note no. 3*. Tunis. Retrieved from: http://www.fao.org/3/ax355e/ax355e.pdf

Reenberg, A. (2012). Insistent Dryland Narratives: Portraits of Knowledge about Human-Environmental Interactions in Sahelian Environment Policy Documents. *West African*

Journal of Applied Ecology, 20, 97–111.

Roy, D. P., M. A. Wulder, T. R. Loveland, C. E. Woodcock, R. G. Allen, M. C. Anderson, D. Helder, et al. 2014. Landsat-8: Science and Product Vision for Terrestrial Global Change Research. *Remote Sensing of Environment*, 145, 154–172. https://doi.org/10.1016/j.rse.2014.02.001

Sheffner, E. J. (1994*).* The Landsat Program: Recent History and Prospects. *Photogrammetric Engineering and Remote Sensing*, 60 (6), 735 – 744

Skinner, E. P. (1988). Sankara and the Burkinabé Revolution: Charisma And Power, Local and External Dimensions. *The Journal of Modern African Studies*, 26(3), 437-455. https://doi.org/10.1017/S0022278X0001171X

Udvardy, M. D. F. (1975). *A Classification of the Biogeographic Provinces of the World*. Morges (Switzerland), International Union for Conservation of Nature and Natural Resources. https://doi.org/10.1017/S0376892900019226

UNCCD. (2021a). *The Great Green Wall Press Kit*. Retrieved from: https://www.unccd.int/sites/default/files/inline-files/OPS%20Press%20kit%20ENG%20%20Version%20-%20Final_0.pdf

UNCCD. (2021b). *The Great Green Wall Initiative.* Retrieved from: https://www.unccd.int/actions/great-green-wall-initiative

USGS (2021a). *Landsat Levels of Processing*. Retrieved from: https://www.usgs.gov/core-science-systems/nli/landsat/landsat-levels-processing?qt-science_support_page_related_con=2 #qt-science_support_page_related_con

USGS (2021b). *What are the best Landsat spectral bands for use in my research?* Retrieved from: https://www.usgs.gov/faqs/what-are-best-landsat-spectral-bands-use-my-research?qt-news_science_products=3#qt-news_science_products

Wu, S., Gao, X., Lei, J., Zhou, N., & Wang, Y. (2020). Spatial and Temporal Changes in the Normalized Difference Vegetation Index and their Driving Factors in the Desert/Grassland Biome Transition Zone of the Sahel Region of Africa. *Remote Sensing*, 12(24), 4119. https://doi.org/10.3390/rs12244119